Los Alamos Proposal Number R-2424-00-0

A proposal for

"Dynamic Inner Magnetospheric Energetic Particle Data and Model Synthesis"

To be performed by:

Los Alamos National Laboratory
Los Alamos, NM 87545

Submitted to:

ROSS-2000 NASA Research Announcement
Living With a Star (LWS) Data Analysis, Theory, and Modeling (DATM)
Jorge Scientific Corporation
Suite 700
400 Virginia Avenue, SW
Washington, DC 20024
(202) 554 2775

Principal Investigator: Reiner H. W. Friedel

Contents

1 Summary of Personnel, Commitments and Cost

1.1 Personnel

R. H. W. Friedel	PI	Los Alamos National Laboratory, Los Alamos, NM
T. E. Cayton	Co-I	Los Alamos National Laboratory, Los Alamos, NM
J .F. Fennell	Co-I	The Aerospace Corporation, El Segundo, CA
S. Bourdarie	Co-I	ONERA, Toulouse, France
D. Boscher	Collaborator	ONERA, Toulouse, France
S. G. Kanekal	Co-I	LASP, Univ of Colorado, Boulder
D. N. Baker	Collaborator	LASP, Univ of Colorado, Boulder

1.2 Proposed Budget

We request a total of $502K funding over three years beginning FY-2001.

Budgets are included for the 3 years of requested support and are in the format required for "Work for Others" proposals from the Los Alamos National Laboratory. Some details for what are on these sheets are for such things as travel and other expenses shown under "Materials and Services". The "other" costs are for possible expenses related to publications of papers (such as page charges).

Travel expenses will be project related, to attend meetings and to visit Collaborators.

The Laboratory is requesting funding for FY2001($166.1k), FY2002($169.7K), FY2003($166.2K).

1.3 Commitments

The funding is to be split up amongst the LANL Investigators; $80K per year, PI R. H. W. Friedel 80%, Co-I T. E. Cayton 20%.

Salammbô code operation, integration and extension is provided by Co-I S. Bourdarie (Science PI) with no-cost support by D. Boscher. Funding is provided by this proposal for several visits to LANL and an extended sabbatical stay of three months in FY2002. Support levels are at $6K, 10$K, $6K for FY 2001 to FY 2003, respectively. These visits will take place under the auspices of the LANL Center of Space Science and Exploration (CSSE). The sabbatical by S. Bourdarie is also supported by his home institution ONERA (see letter of commitment).

SAMPEX data, analysis and model integration is provided by Co-I S. G. Kanekal of Lab. for Atmos. and Space Physics (LASP), University of Colorado, with no-cost support by D. N. Baker. This is a LANL/University colaboration funded though this proposal at $30K per year.

HEO data, analysis and model integration is provided by Co-I J. F. Fennell of The Aerospace Corporation. This contribution is budgeted at $25k per year.

2 Scientific/Technical/Management

Dynamic Inner Magnetospheric Energetic Particle Data and Model Synthesis

2.1 Abstract

The harsh radiation environment in the inner magnetosphere up to geosynchronous orbit is of major concern to an ever increasing amount of space hardware. The energetic particle fluxes from these regions are of further concern to regions of low-Earth orbit such as occupied by the International Space Station, especially during disturbed conditions. While the average or quiescent conditions of the energetic particle population are fairly well characterized, the dynamics during magnetic storms are severely under-sampled. The underlying processes responsible for the large variability in the observed behavior of the relativistic electron component in particular, are still a matter of intense scientific debate.

We intend here to use a theoretical model (Salammbô) to extend and combine existing energetic particle measurements to interpolate in L and to extrapolate the energy range. Combining both measurements and model enables us to increase both the spatial and temporal resolution of the data, and allows us to define time-dependent maps of the radiation belts, both for now-casting and research purposes.

We expect the results of this proposal to answer the following specific questions:

1. *What is the dynamic radiation environment during magnetic storms at the International Space Station altitude?*
2. *What are the global dynamic inner radiation belt conditions during active times?*
3. *Are internal acceleration mechanisms needed to explain relativistic electron dynamics during magnetic storms?*
4. *What is the optimum number of spacecraft and minimum instrument specification needed for the LWS Radiation Belt Mapper?*

Salammbô is a sophisticated particle transport code which has been used successfully to reproduce the global radiation belt dynamics for energetic electrons and protons, using relatively few inputs such as geosynchronous particle flux data as a boundary condition and Kp. In the absence of other data inputs, Kp is used as a scaling proxy for radial diffusion, plasmapause location and wave activity. Salammbô also includes a small-scale recirculation process which has been used to model the dynamics of relativistic electrons.

Data is provided by DOE/DOD geosynchronous, GPS, HEO, and SAMPEX satellites. These satellites carry energetic particle instrumentation which provide almost total coverage of the magnetosphere ranging in L from 1.1 to 8 and at altitudes from low earth to beyond geosynchronous. These spacecraft, all currently operational, provide nearly continuous data over almost a decade. They form the first proper inner magnetospheric constellation and are an ideal testbed for future constellation-type missions such as envisioned by the Living with a Star Program. The resources of this existing constellation and its basic operation are not only assured for the foreseeable future, but can be used by the Living with a Star Program at no operational cost.

2.2 Introduction

One of the important aspects of the inner magnetospheric plasma environment is the time-dependent mapping of the trapped, high energy radiation belts. During magnetic storms, it was shown that the radiation belts are highly dynamic [20], with relativistic electron fluxes being enhanced more than a thousand-fold in mere minutes [35]. If a high energy solar proton event accompanies the storm (as is often the case), then new relativistic protons can be trapped in the radiation belts for long periods, such as after the major

1991 event [24].

Apart from drastically increasing the levels of energetic particles, magnetic storms also lead to a dramatic radial shift inward of the peak of these particle fluxes, from quiet time position near $L = 4.5$ to as little as $L = 2.5$ [41]. This would bring the mirror points of this trapped population to latitudes occupied by low-Earth orbiting spacecraft and facilities such as the International Space Station (ISS). Increased energetic electrons dominate the radiation dose in most Earth orbits, and are an obvious concern for human habitation in space.

From a purely hardware point of view, such dynamics can lead to spacecraft surface and internal charging and may lead anomalous behavior. Single event effects due to high energy protons can induce non reversible degradation on electronic devices (such as latchup) and discharges due to energetic electrons via the process of deep dielectric discharge may lead to operational failures [4].

While the detailed global knowledge of the dynamic behavior of energetic particles is of obvious importance to spacecraft and or humans operating in that environment, the understanding of the inner magnetospheric particle population dynamics is also an important scientific question.

Many recent studies of geomagnetic storms [6; 38; 37; 27; 5; 7; 8; 21; 28; 26; 12] have investigated the dynamical behavior of relativistic electrons. Observations at geosynchronous orbit, have revealed that relativistic electron flux increases occur several days after the onset of a magnetic storm, and that there is a poor correlation between the size and/or duration of the increase with other storm-time indicators such as Dst, Kp. The correlation with solar wind speed, on the other hand has been well established since the 1970s' [33]. In addition, the orientation of the interplanetarty magnetic field may also be an important factor [32; 11]. Theoretical models have proposed mechanisms such as radial diffusion, wave-particle interaction and impulsive shock acceleration as underlying processes. Some of the more detailed suggestions include ULF wave heating [29], simple diffusion and heating by conservation of the first adiabatic invariant [23], acceleration by substorms [25] and recirculation at the plasmapause location [15]. Currently, the situation remains unclear as to whether a given mechanism or several processes operate simultaneously and as to the nature of the relationship of these on external factors.

Observational studies use data from single or multiple points in space and are unable to rigorously distinguish between possible acceleration processes. These studies are limited due to insufficient coverage of measurements [21]. To have a good representation of what really happens during magnetically active periods, several spacecraft have to be at the "right location" at the "right time" which is rarely the case.

With the use of physical models of radiation belts it is possible to interpolate between measurements (particularly in L) as well as extrapolate taking into account the limited channel number and energy range of instruments. Combining both measurements and theoretical model is a good way to increase the spatial and temporal resolution of measurements to produce time-dependent maps of the radiation belts, both for now-casting capabilities and as a tool for further research into mechanisms and causes.

We intend to produce such a global model of the energetic radiation belt by combining the existing data (GEO, GPS, HEO, and SAMPEX) with a mature radiation belt model, the Salammbô code. This enterprise will provide a test bed for forthcoming constellation-type projects wherein the use multi- spacecraft data in combination with physical models to characterize the global environment is planned. This is particularly applicable to the LWS radiation belt mapper. Lessons learned here are directly applicable to both the planning and operation of the radiation belt mapper. Our study will aid in delineating the requisite number of spacecraft and types of measurements needed to produce time-dependent maps with acceptable accuracy. Thus, it will greatly aid in maximizing scientific output while minimizing the cost of a mission such as the LWS radiation belt mapper.

The Salammbô code (details in section 2.4) has been run at Los Alamos National Laboratory for selected cases and is supported by one of our Co-Investigators, Dr. S. Bourdarie. As part of this proposal it is planned for Dr. Bourdarie to spend a 3-month sabbatical at Los Alamos National Laboratory. Salammbô routinely uses LANL geosynchronous energetic particle data as input for its boundary conditions.

The use of GEO, GPS, HEO, and SAMPEX (details in section 2.3) data has several advantages. Firstly, GEO,

GPS, HEO, and SAMPEX are all currently operational, with considerable expertise in their data analysis in place (PI R. Friedel and Co-I T. Cayton at LANL, Co-I J. Fennell at Aerospace, Co-Is D. N. Baker and S. G. Kanekal at LASP, Colorado). The data from these missions will be available for the foreseeable future, at no cost to the LWS program. Secondly, the GEO data together with Kp and Salammbô already provide the capability for limited now-casting of the energetic radiation belts. Finally, until the operation of the LWS radiation belt mapper, these data together with the model-interpolation will be the only system in place that can provide near-real time environmental data to the ISS (and other operational spacecraft).

2.3 Missions and Data

Mission	Orbit	e^- range	p^+ range
LANL GEO	geo	.05–10 MeV	.075–60 MeV
LANL GPS	meo	.2–10 MeV	9–60 MeV
HEO	petal	.13–5 MeV	80 to 360 keV
			6.5–30 MeV
SAMPEX	leo	.4–30 MeV	4–80 MeV

2.3.1 LANL GEO data

Energetic particle data is provided by LANL SOPA [36] and ESP [31] instruments on-board geosynchronous satellites. This provides energy coverage from 50keV – 10MeV for electrons and 75keV – 60MeV for protons. Even though these satellites do not carry on-board magnetometers, it is possible to extract pitch angle information from the data by indirect means. From spin-resolved data the magnetic field direction can be determined by finding the axis of gyrotropy of the particle distribution measured in spacecraft coordinates. This is now being done for these data on a routine basis at LANL. Having the full pitch angle information available is invaluable as an input to Salammbô, which uses these data as a boundary condition.
Data are available from up to four geosynchronous local times at any given time, with a 15+ year database and assured continuing operation. Some of the data is also available in near real-time, which is essential for any now-casting system.

2.3.2 LANL GPS data

The Global Positioning System (GPS) constellation consists of 24 operating satellites with circular orbits (radius 4.2 R_E, 55^o inclination, 12 hour period, $L : 4 \rightarrow 8$ every 3 hours). Since 1990, up to 4 GPS satellites at any given time are equipped with BDD-II particle detectors [2; 18] which measure energetic particles in the range 200 keV - 10 MeV for electrons and 9 MeV - 60 MeV for protons.
In the time frame of this proposal, at least 2 further GPS satellites with LANL energetic particle detectors are scheduled to be launched.

2.3.3 AEROSPACE HEO data

The three HEO spacecraft make up a single petal with the satellites following each other around that petal. The HEO's have low perigee($\sim$ $600 - 900$ km), high apogee ($\sim$ 7.2Re) 63^o inclinations, and a twelve hour period. We obtain continuous coverage of the regions for $L > 4$ for two HEO's and full orbit coverage for the third. The three satellite HEO constellation was in place from December 1997 forward. The earliest HEO data starts in July 1994. One of the HEO satellites made plasma measurements from mid 1995 to 1998. Those observations could help define the seed population at large L since the HEO's sample from the tail lobe down to lower L values. The third HEO satellite provides a direct measure of precipitating fluxes in the low altitude perigee regions, but at the 63^o latitude.
The HEO measurements cover the energy range from 130 keV to 5 MeV for electrons, 80 to 360 keV protons, and 6.5 to 30 MeV protons. In addition they measure the actual radiation dose behind spherical shields equivalent to 12 to 400 mils Al for $L > 4$ and 12 to 125 mils Al over the full orbit. The HEO2 plasma instrument measures electrons and protons in the 100 eV to 30 keV range [11; 19]

2.3.4 SAMPEX data

SAMPEX, the first of the Small Explorers (SMEX) is a low Earth orbiting satellite (520x675 Km at, inclination 82^o, period $\sim$90 minutes) operating since 3 July 1992. The high inclination of SAMPEX allows the sensors onboard to sample almost all L shells 4 times an orbit. The satellite is usually zenith pointing with

extended periods of cart-wheel spin enabling pitch angle separation. SAMPEX provides information about highly energetic particles that are either precipitating or mirror at the satellite altitude.
There are four sensors onboard all measuring energetic particles (HILT, MAST, PET and LICA [3]), with time resolutions ranging from milliseconds to 6 seconds. Here we mainly use the PET detector, a solid state telescope providing measurements of electrons of energy > 0.4 MeV to 30 MeV. The ELO channel is particularly important to this study measuring the relativistic electron fluxes in the range 2.0 to 6.0 MeV. Two other channels on the HILT detector also measure electrons of energies > 1.0 MeV and > 3.0 MeV. In addition protons of energy from 4.0 to 80.0 MeV are also measured.

2.4 The Salammbô Code

Salammbô is a comprehensive modeling effort for the radiation belts, based on classical diffusive theory [40; 39]. The Salammbô code is a sophisticated particle diffusion code that models physical processes in the inner magnetosphere in terms of equivalent diffusion coefficients. It has been used to model the main ring current protons [13] and electrons [16] and has been extended to cover dynamic times [17; *Vacaresse et al.*; 15].

The code is also successful in modeling the relativistic electron belt as well as the inner proton belt. Salammbô models processes that are interior to the magnetosphere for relativistic electrons (for example wave-particle interaction near the plasmasphere) and for high energy proton (solar proton trapping).

The code is 3-D in phase space (magnetic moment, 2nd invariant, L), in a dipole geometry, and assumes there are no variations in longitude. This is a valid assumption for relativistic electrons and high energy protons, since each drift shell is populated uniformly on timescales of a drift orbit ($\sim$ 10's of minutes). Details of the electron and proton model have been published [9; 10]. It is important to note that the code does not incorporate electric field convection. However, for the range of energies important to ISS and other space systems, from the perspective of damage and mission lifetime, convection is not important. An extension of the model to 4-D (mag moment, 2nd invariant, L, MLT) has been used to model the detailed dynamics during storms [17]. This version of the code is too computationally intensive for anything but case studies. For the routine running of the model we will use the 3-D code. Input parameters need to be mapped into the code's coordinate system using realistic magnetic field models, and any outputs need to be mapped back into fluxes in the same field models(see section 2.5).

One of the strengths of the Salammbô code are the limited input data needed: Data for particles fluxes at an outer boundary and Kp - this is sufficient to reproduce all the important dynamic features observed in the real magnetosphere.
For detailed matching of the model to reality, higher time resolution input parameters may be needed. Kp in the model is a proxy for several processes - it scales the diffusion coefficients for radial diffusion by magnetic and electric perturbation fields, the magnetopause position as a loss mechanism, the location of the plasmapause for wave activity and the magnitude of the wave activity itself. For Kp we can substitute the midnight boundary index (MBI) which has a direct relation to Kp and sub-hour resolution. Wherever possible, we will investigate the use of the highest resolution solar wind data (ACE, IMP) as input parameters for these individual processes. However, having Kp as a "fall-back" option is useful as the solar wind data may not always be available. Solar wind parameters will also be used to specify the magnetopause position for drift shell day side losses.

The currently used boundary fluxes in the electron model model derive from LANL geosynchronous observations, which limits the valid range of the model to geosynchronous inward. For the uses intended in this proposal, i.e. get a good coverage for electron and proton belts at all L up to $L = 8$, we intend to add LANL GPS and AEROSPACE HEO data.

The Salammbô code cannot perform a global simulation of all the magnetospheric plasma dynamics (such as done by MHD codes or global convection models such as the Rice Convection Model). For our purpose here, which is to concentrate on the highly energetic particle population (which is of central importance to Space Weather), a comprehensive model is not needed. Relativistic electrons play an insignificant role from the perspective of total energy contribution to the dynamics.

2.4.1 Details on the electron model

For electrons the code includes the deceleration of particles by free and bounded thermospheric and ionospheric particles, pitch angle diffusion by wave-particle interactions [30; 1], Coulomb interactions, losses due to Synchrotron emissions and radial diffusion by magnetic and electric field perturbations. A flowchart of the electron code is given in Figure 1.

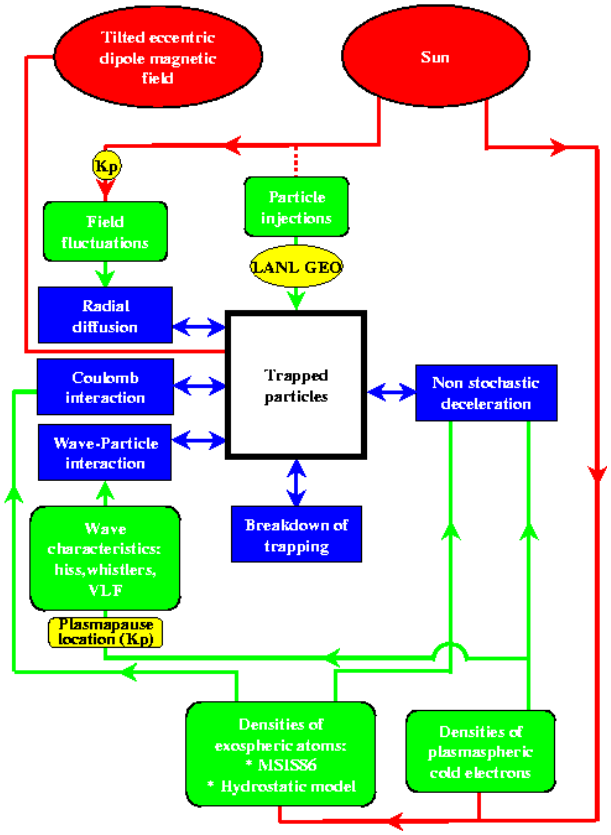

Figure 1: The Salammbô Code: The electron radiation belt model.

In this code, no specific parts were included for the modeling of relativistic electrons - rather, the relativistic electron acceleration is a natural outcome of the features included in the code, which also reproduce the features of the main ring current. Detailed investigation of the code operation has indicated that the following process is operating:

20-50 keV electrons diffuse inward from the model boundary (very rapidly at storm onset) and are adiabatically heated to 100-200 keV. Near the plasmapause, the location of strong magnetospheric hiss and other waves, these electrons are further heated and scattered, enabling them to undergo a recirculation loop through this region. Each loop (pitch angle scattering and diffusion) enables a given electron to traverse the acceleration region many times. In contrast to the large scale diffusion proposed by earlier authors [22], this is a small-scale process in the vicinity of the plasmapause [14]. This recirculation was NOT imposed on the code but is a natural result of the modeled pitch angle and radial diffusion.

The plasmapause, in the model, effectively defines the source region for relativistic electrons. This location is typically near 4 R_e, but can vary strongly during active times. No new electrons are produced inside the model outer boundary - recirculation is just a process that energizes electrons from ~100's keV to MeV. As the plasmapause moves during a storm the recirculation takes place over a large L range. Electrons accelerated here then diffuse inward and outward during the storm recovery at nominal rates, which can explain their delayed appearance at geosynchronous altitudes.

Salammbô makes assumptions about the radial gradient of phase space density. Depending on Kp for radial diffusion and wave-particle activity for recirculation, the radial profile can be positive or negative.

An example of the code output is given in Figure 2. The bottom panels shows the time series of Kp (which is one of the inputs) for the period 21 September to 02 October, 1998. A magnetic storm occurs on 24 September as indicated by extremely large Kp values (above 8). The next panels show the behavior of 0.1, 0.4 and 1.6 MeV electrons. At storm onset lower energy electrons are rapidly diffused inward to $L = 3$ to 5, and adiabatically heated to 100 keV, which forms the source population that is then further accelerated near the plasmapause ($L \sim 4$). Relativistic energies (top panel) first build up in this region before diffusing outwards to higher L.

The actual time history of the fluxes observed at any point in space (geosynchronous being the most important given the density of satellite operations there) depend on the complex interrelation of several factors:

1. Variation of the source population at the plasmapause - for relativistic electrons, 100-200 keV. This depends on the variation of the boundary spectrum and the magnitude of electron diffusion coefficients during storm onset.
2. Magnitude of radial diffusion coefficient through-

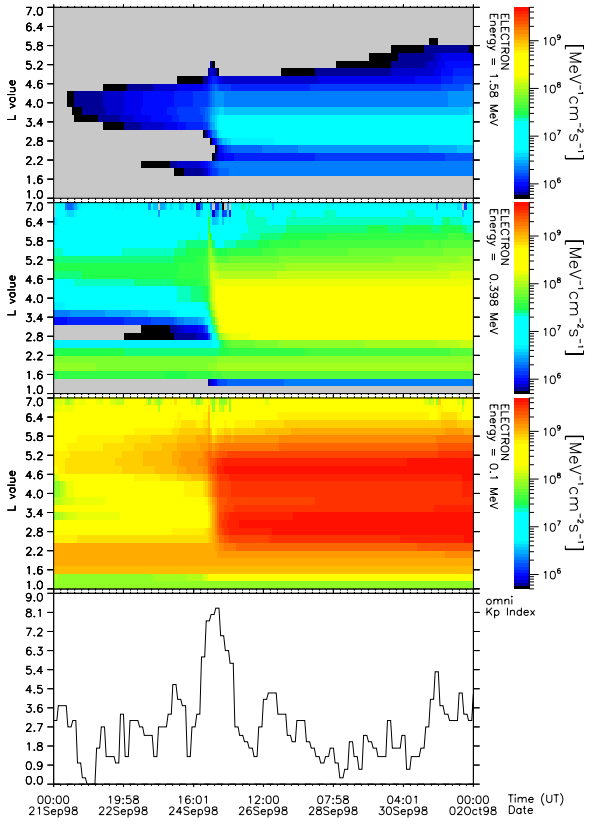

Figure 2: Salammbô output for modeling the electron radiation belts with static boundary conditions, static plasmapause location and a time series of Kp as input.

out storm.

3. Plasmapause location and time history during storm and recovery.
4. Level of wave activity throughout storm.
5. Loss processes and range during storm onset.

For relativistic electrons, storm onset acts like a large-scale loss process, which is fairly simple to model. Due to their fast drift times (10's of minutes) even short-lived compressions of the dayside magnetopause can effectively empty out most relativistic electrons at storm onset. The radial range of this loss is given by the position of the magnetopause (R_{MP}) - how far that moves inwards at storm onset. This can be predicted from upstream solar wind measurements, which are routinely available from solar wind monitors (ACE for current and future use, WIND and IMP for past use):

$$R_{MP} = \frac{(2B_s)^{1/3}}{(2\mu_o \rho V^2)^{1/6}} \qquad (1)$$

where B_s is the dipole magnetic field strength at 1 R_E, V is the solar wind speed and ρ the solar wind density. We can use this information to re-initialize the model correctly at storm onset.

2.4.2 Details on the proton model

Compared to electrons, for protons pitch angle diffusion is neglected, whereas charge exchange is taken into account.

In the proton model three different sources are considered. First low energy protons are accelerated from the outer L boundary limit to the inner part of the belt by enhanced radial diffusion. Second high energy protons are created by CRAND process especially at low altitude. This source term is solar cycle dependent. The third source is a sporadic one and is due to solar flares. Time dependent magnetospheric shielding has been introduced, controlling the radial access of flare protons to the inner magnetosphere. This access limit can be as low as $L = 2.5$, as during the March 1991 event. If a geomagnetic storm occurs at the same time, then those new particles can be trapped because they can diffuse inward due to enhanced radial diffusion.

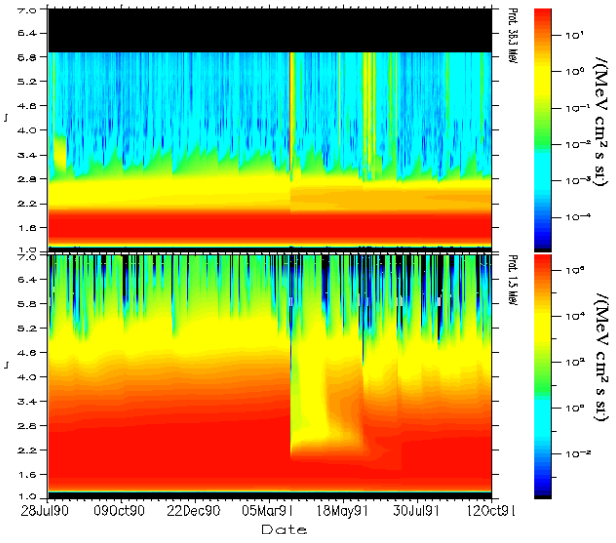

Figure 3: Salammbô output for modeling the energetic proton radiation belts.

An example of the code output is given in Figure 3. The fourteen months plotted here correspond to the CRRES period. The top panel shows high energy protons (36.3 MeV) in a L versus time map. The effect of solar proton events can be seen at different times. Depending on the simultaneous presence of a

storm, particles can be trapped and form a second belt. The lower panel presents 1.5 MeV protons and clearly shows particle losses at large L values due to magnetopause shadowing.

2.5 Method

We describe here the tools needed for comparing model and data, and the rationale behind our approach in combining model and data to produce the best time-dependent representation of the energetic radiation belts. Finally we show how our model can be used as a planning tool for constellation-type missions such as the Radiation Belt Mapper of LWS.

2.5.1 Data formatting

In order to provide input to the model or to compare data to model we need to be able to fold data and model into the same coordinate system (magnetic moment, 2nd invariant, L).

The main spatial coordinate is L - it is well known that trapped energetic particles follow magnetic drift shells as given by the McIlwain L parameter. These drift shells are dependent on magnetic activity; to have a consistent L value we will use the same time dependent magnetic field model for each spacecraft to compute L of the measurement. We propose to use the various Tsyganenko models (T87, T89, T96) and Olson-Pfitzer model together with the needed time-dependent input parameters. Some iteration on model use will be needed until the best one is found for this purpose.

When pitch-angle informations are available (GEO data) we can compute the magnetic moment and 2nd invariant directly. If no or limited pitch angle information is available (HEO, GPS) we have two options:
a) To assume some sample pitch angle distributions (such as $j \sim \sin^{2s}\alpha$, with s taken from published results. GPS analysis at LANL has shown that $s \sim 0.5$ [34] is a "good" assumption for GPS data).
b) To extract from the full distribution function represented in the Salammbô code the data as specified by the instrument response. This in effect allows us to fly a virtual instrument though the model.
We intend to pursue and test both these methods.

2.5.2 Model/data synthesis

We intend here to use the model/data synthesis for two interrelated tasks:

(a) Model validation / test against data

Here we use our data as boundary conditions (input) to the Salammbô code, run the code and test the results against data inside this boundary.

Initially the boundary condition will be from the LANL GEO data, with extension to $L = 8$ using GPS and HEO data. We run the code dynamically updating the boundary conditions and the other inputs needed (Kp, Dst, see section 2.4) at each time step.

We will then use data from other locations inside geosynchronous to test the validity of the model. This uses GPS, HEO and SAMPEX data, with GPS used down to $L = 4$, HEO below that and both HEO and SAMPEX at low-Earth orbit altitudes. This allows us determine to what extend the physical processes in the model are a good and/or sufficient representation of reality. This is of interest in particular to the issue of relativistic electron dynamics. Is the recirculation process modeled here sufficient to reproduce all the dynamics? Or are some of the other processes mention in Section 2.2 more important?

(b) Combination of model and data

Here we intend to increase the input parameters into the model to not only include boundary conditions and Kp and Dst, but incorporate as many measurements as possible.

When running the Salammbô code, as outlined above, at each time when a measurement is available on the LANL GEO and GPS, AEROSPACE HEO and SAMPEX satellites, the corresponding point in the Salammbô [M, J, L] grid will be set to the data value. We then allow the operation of the diffusion code to self-consistently "fill in" the correct data between the imposed data points between time steps. In this way we can interpolate and extrapolate between all the measurements, as well as increasing the Salammbô accuracy even if physical processes parameterization is not available all the time.

This process can work if the difference between the model grid points and the data values is not too great, and the parameterization of the diffusion coefficients is reasonable. Since this parameterization comes from

statistical, average conditions for a given activity level, we can use data to "correct" the model in order to provide a better real-time fit. This process in effect imposes a multi-point, spread out time varying boundary condition on the model; by restricting the region in which the model needs operate by itself we can improve the overall accuracy of the model in a substantial way.

Either method will yield a representation of the global, time-dependent energetic particle radiation belts - either as Salammbô-only output or as a combined interpolated Salammbô / data output.

2.5.3 Model Mapper

Given a valid, data-tested model as a function of time, we can then extract from the results global maps of the time dependent electron and proton flux levels in the inner magnetosphere. This involves the reverse mapping from the model coordinates (magnetic moment, 2nd invariant, L) back into real space, using the same magnetic field models as used in mapping input data to model coordinates.

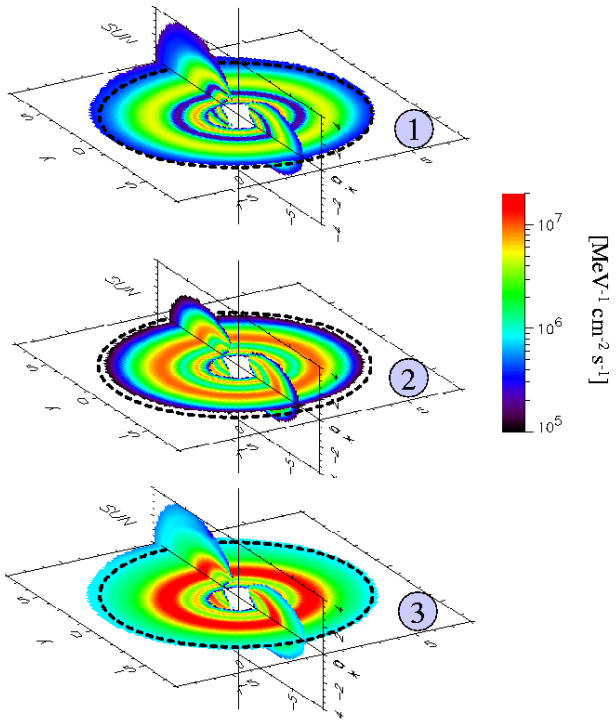

Figure 4: Salammbô output for modeling the energetic proton radiation belts.

Figure 4 shows a sample of the relativistic electron (1 MeV) map at different times during the September 1998 storm.The first view is just before the storm, the second one is when Kp is maximum and the third is during the recovery phase, two days after the storm onset.

In addition, given any orbit we can fly a virtual spacecraft through this model to produce the radiation levels at that spacecraft. This is of particular interest to the ISS or any operating spacecraft without particle instruments onboard. Figure 5 shows a sample of the relativistic electron fluxes at 400 km altitude (the ISS orbit).

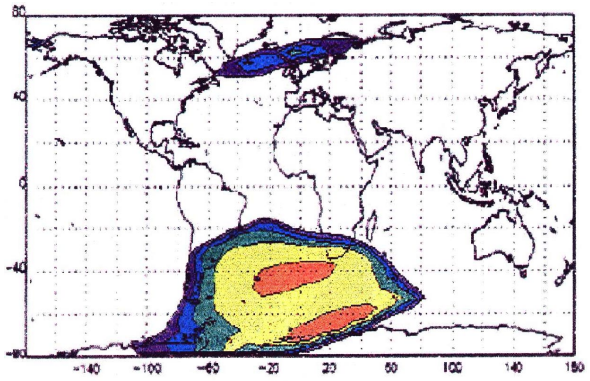

Figure 5: Salammbô fluxes at ISS orbit altitude. Red is most intense fluxes.

2.5.4 Constellation analysis

Once the mapper has been set up, we can investigate the effect on the map accuracy of limiting the number of data inputs. This of great interest for the LWS Radiation Belt mapper mission, because we can then determine the minimum number of spacecraft required for a good definition for the radiation belts. The idea here is to remove a given spacecraft from the model/data synthesis runs, and then to compare the data of the removed spacecraft to the model predictions for that location. We intend to test the effect on the radiation belt map accuracy of several factors:

1. Data location
2. Data quality (pitch angles available?)
3. Data time resolution
4. Data energy resolution.

2.6 Proposed tasks

We propose a three year program to develop and use the scientific and operational tools for the proposed model/data synthesis:

1. FY 2001
   (a) Choice and collection of data (including data formatting and intercalibration) and model inputs for case studies (e.g. storm periods of the GEM inner magnetosphere campaign).
   (b) Radial extension of Salammbô boundary condition input to $L = 8$.
   (c) Set up high resolution Salammbô code for case studies.
   (d) Model storm run validation against all possible in-situ observations.
   (e) Presentation of first case studies at conferences.
2. FY 2002
   (a) Three month sabbatical by S. Bourdarie at LANL, extension of Salammbô to take arbitrary boundary condition input (model/data synthesis).
   (b) Refinement/extension of physical processes modeled to improve validation, iterate.
   (c) Case studies of Salammbô model/data synthesis runs. Production of highest quality radiation belt maps form these runs.
   (d) Publication of first results
3. FY 2003
   (a) Mapping analysis (accuracy versus satellite number).
   (b) Extended storm studies using the Salammbô model/data synthesis runs for a variety of magnetic storms / disturbed times.
   (c) Radiation Belt Mapper planning study: determine minimum constellation and instruments needed to specify radiation belt globally.
   (d) Publication of model/data synthesis radiation belt maps.

2.7 Summary

We propose here to use a large set of existing energetic particle data in the inner magnetosphere in combination with a sophisticated radiation belt transport model to obtain for the first time a time-dependent, accurate and global representation of the radiation belts.

The benefit of this proposal to the LWS program are two-fold. First, using a typical run of the current version of the Salammbô code which gives the full radiation belt distribution for high energetic protons and relativistic electrons during active periods it will be possible to simulate spacecraft orbits and to determine their radiation environment, such as for the International Space Station.

Second, with data/model synthesis proposed here we can not only improve the accuracy of our model, but also investigate the effects of spacecraft density, limitations of instrumentation and data time resolution on the accuracy of our maps. This will be the ideal planning tool for the proposed Radian Belt Mapper mission. In the process of performing this we we will also develop the tools that will be needed to assimilate data from constellation type missions - data from the LWS missions can be seamlessly integrated into the structures set up for this study.

The time-dependent radiation belt maps here also have scientific application for the investigation of storm dynamics. Global specification of the phase-space density will enable us to address the outstanding issues in relativistic electron acceleration / transport during magnetic storms.

3 Miscellaneous Information

Los Alamos National Laboratory is a Federally Funded Research and Development Center (FFRDC) and, as such, is exempt from providing certifications regarding Drug Free Workplace, Debarment and Suspension, and Lobbying. No part of this proposal is being submitted to other agencies.

4 List of related publications

References

[1] Abel, B., and R. M. Thorne, Electron scattering in Earth's inner magnetosphere, 1. Dominant physical processes, *J. Geophys. Res.*, *103*, 2385–2396, 1998.

[2] Argo, H. V., D. N. Baker, R. D. Belian, L. K. Cope, and P. R. Higbie, The BDD: A dosimeter for the global positioning system, *Tech. Rep. LA-8421-MS*, LOS ALAMOS NATIONAL LABORATORY, LOS ALAMOS, NM 87545, USA, 1980.

[3] Baker, D. N., G. M. Mason, O. Figueroa, G. Colon, J. Watzin, and R. M. Aleman, An overview of the solar, anomalous, and magnetospheric particle explorer (SAMPEX) mission, *IEEE Trans. Geosc. Remote Sens.*, *31*, 531–541, 1993.

[4] Baker, D. N., J. H. Allen, S. G. Kanekal, and G. D. Reeves, Disturbed space environment may have been related to pager satellite failure, *EOS Trans. AGU*, *79*, 477, 1998a.

[5] Baker, D. N., X. Li, J. Blake, and S. Kanekal, Strong electron acceleration in the Earths magnetosphere, *Adv. Space Res.*, *21*, 609–613, 1998b.

[6] Baker, D. N., et al., Recurrent geomagnetic storms and relativistic electron enhancements in the outer magnetosphere : ISTP coordinated measurements, *J. Geophys. Res.*, *102*, 14,141–14,148, 1997.

[7] Baker, D. N., et al., A strong CME-related magnetic cloud interaction with the Earth's magnetosphere: ISTP observations of rapid relativistic electron acceleration on May 15, 1997, *Geophys. Res. Lett.*, *25*, 2975–2978, 1998c.

[8] Baker, D. N., et al., Coronal mass ejections, magnetic clouds, and relativistic magnetospheric electron events : ISTP, *J. Geophys. Res.*, *103*, 17,279–17,291, 1998d.

[9] Beutier, T., and D. Boscher, A three-dimensional analysis of the electron radiation belt by the salammbô code, *J. Geophys. Res.*, *100*, 14,853–14,861, 1995.

[10] Beutier, T., D. Boscher, and M. France, A three-dimensional analysis of the proton radiation belt by the salammbô code, *J. Geophys. Res.*, *100*, 17,181–17,188, 1995.

[11] Blake, J. B., D. N. Baker, N. Turner, K. W. Ogilvie, and R. P. Lepping, Correlation of changes in the outer-zone relativistic-electron population with upstream solar wind and magnetic field measurements, *Geophys. Res. Lett.*, *24*, 927–929, 1997.

[12] Boscher, D., and S. Bourdarie, Transport of energetic particles in the magnetosphere, *AGU monograph*, 2000, submitted.

[13] Boscher, D., S. Bourdarie, R. Friedel, and A. Korth, Long term dynamic model for low energy protons, *Geophys. Res. Lett.*, *25*, 4129–4132, 1998.

[14] Boscher, D., S. Bourdarie, R. M. Thorne, and B. Abel, Influence of the wave characteristics on the electron radiation belt distribution, *Adv. Space Res.*, *26 (#1)*, 163–166, 2000.

[15] Boscher, D., S. Bourdarie, R. M. Thorne, and B. Abel, Toward nowcasting of the electron belt, *AGU monograph*, 2000, submitted.

[16] Bourdarie, S., D. Boscher, T. Beutier, J. A. Sauvaud, and M. Blanc, Magnetic storm modeling in the Earth's electron belt by the salammbô code, *J. Geophys. Res.*, *101*, 27,171–27,176, 1996.

[17] Bourdarie, S., D. Boscher, T. Beutier, J.-A. Sauvaud, and M. Blanc, Electron and proton radiation belt dynamic simulations during storm periods: A new asymmetric convection-diffusion model, *J. Geophys. Res.*, *102*, 17,541–17,552, 1997.

[18] Cayton, T. E., D. M. Drake, K. M. Spencer, M. Herrin, T. J. Wehner, and R. C. Reedy, Description of the BDD–IIR: Electron and proton sensors on the GPS, *Tech. Rep. LA-UR-98-1162*, Los Alamos National Laboratory, Los Alamos, NM 87545, USA, 1998.

[19] Fennell, J. F., J. B. Blake, J. L. Roederer, R. Sheldon, and H. E. Spence, Tail lobe and open field line region entries at mid to high latitudes, *Adv. Sp. Res.*, *20*, 431–435, 1997.

[20] Friedel, R. H. W., and A. Korth, Long-term observations of keV ion and electron variability in the outer radiation belt from CRRES, *Geophys. Res. Lett.*, *22*, 1853–1856, 1995.

[21] Friedel, R. H. W., et al., A multi-spacecraft synthesis of relativistic electrons in the inner magnetosphere using LANL, GOES, GPS, SAMPEX, HEO and POLAR, *Radiat. Meas.*, *18*, 589–597, 1999.

[22] Fujimoto, M., and A. Nishida, Energization and anisotropization of energetic electrons in the Earth's radiation belt by the recirculation process, *J. Geophys. Res.*, *95*, 4265–4270, 1990.

[23] Hilmer, R. V., G. P. Ginet, and T. E. Cayton, Enhancement of equatorial energetic electron fluxes near $L = 4.2$ as a result of high speed solar wind streams, *J. Geophys. Res.*, *105*, 23,311–23,322, 2000.

[24] Hudson, M. K., A. D. Kotelnikov, X. Li, I. Roth, M. Temerin, J. Wygant, J. B. Blake, and M. S. Gussenhoven, Simulation of proton radiation belt formation during the march 24, 1991 SSC, *Geophys. Res. Lett.*, *22*, 291–294, 1995.

[25] Ingraham, J. C., R. D. Belian, T. E. Cayton, R. Christensen, R. H. W. Friedel, M. M. Meier, G. D. Reeves, and M. Tuszewski, Substrom injection of relativistic electrons to geosynchronous orbit during magnetic storms: A comparison of the march, 24, 1999 and march 10, 1998 storms, AGU Spring Meeting, Washington D.C.May 30 – June 3, 2000.

[26] Kanekal, S. G., D. N. Baker, J. B. Blake, B. Klecker, G. M. Mason, and R. A. Mewaldt, Magnetospheric relativistic electron response to magnetic cloud events of 1997, *Adv. Space Res.*, *25 (#7/8)*, 1387–1392, 2000.

[27] Li, X. L., et al., Energetic electron injections into the inner magnetosphere during the January 10–11, 1997 magnetic storm, *Geophys. Res. Lett.*, *25*, 2561–2564, 1998.

[28] Li, X. L., et al., Sudden enhancements of relativistic electrons deep in the magnetosphere during May, 1997 magnetic storm, *J. Geophys. Res.*, *104*, 4467–4476, 1999.

[29] Liu, W. W., G. Rostoker, and D. N. Baker, Internal acceleration of relativistic electrons by large-amplitude ULF pulsations, *J. Geophys. Res.*, *104*, 17,391–17,407, 1999.

[30] Lyons, L. R., R. M. Thorne, and C. F. Kennel, Pitch-angle diffusion of radiation belt electrons within the plasmasphere, *J. Geophys. Res.*, *77*, 3455–3474, 1972.

[31] Meier, M. M., R. D. Belian, T. E. Cayton, R. A. Christensen, B. Garcia, K. M. Grace, J. C. Ingraham, J. G. Laros, and G. D. Reeves, The energy spectrometer for particles (ESP): Instrument description and orbital performance, in *Workshop on the Earth's Trapped Particle Environment, AIP Conf. Proc.*, edited by G. D. Reeves, vol. 383, pp. 203–210, Am. Inst. of Phys., Woodbury, N. Y., 1996.

[32] Paulikas, G. A., and J. B. Blake, Modulation of trapped energetic electrons at 6.6 R_E by direction of interplanetary magnetic-field, *Geophys. Res. Let.*, *3*, 277–280, 1976.

[33] Paulikas, G. A., and J. B. Blake, Effects of the solar wind on magnetospheric dynamics: Energetic electrons at the synchronous orbit, in *Quantitative Modeling of the Magnetospheric Processes*, edited by W. Olson, vol. 21 of *Geophys. Monogr. Ser.*, pp. 180–202, AGU, Washington D.C., 1979.

[34] M. G. Tuszewski, T. E. Cayton, R. H. W. Friedel, and J. C. Ingraham, Apparent electron flux limits from GPS satellite data, Talk, AGU Fall Meeting, San Francisco, USA, 1999.

[35] Reeves, G. D., Relativistic electrons and magnetic storms: 1992-1995, *Geophys. Res. Lett.*, *25*, 1817–1820, 1998.

[36] Reeves, G. D., R. D. Belian, T. C. Cayton, M. G. Henderson, R. A. Christensen, P. S. McLachlan, and J. C. Ingraham, Using Los Alamos geosynchronous energetic particle data in support of other missions, in *Satellite-Ground Based Coordination Source Book*, edited by M. M.Lockwood and H.J.Opgenoorth, pp. 263–272, ESA Publications, ESTEC, Noordwijk, The Netherlands, 1997.

[37] Reeves, G. D., R. Friedel, M. Henderson, D. Belian, M. Meier, D. Baker, T. Onsager, and H. Singer, The relativistic electron response at geosynchronous orbit during the January 1997 magnetic storm, *J. Geophys. Res.*, *103*, 17,559–17,570, 1998a.

[38] Reeves, G. D., et al., The global response of relativistic radiation belt electrons to the January 1997 magnetic cloud, *Geophys. Res. Lett.*, *25*, 3265–3268, 1998b.

[39] Schulz, M., The magnetosphere, *Geomagnetism*, *4*, 87–293, 1991.

[40] Schulz, M., and L. J. Lanzerotti, *Particle Diffusion in the Radiation Belts*, Springer-Verlag, New York, 1974.

[41] Tverskaya, L. V., N. N. Pavlov, J. B. Blake, R. S. Selesnick, and J. F. Fennell, Predicting the L-position of the storm-injected relativistic electron belt, *Adv. Space Res*, in press, 2000.

[*Vacaresse et al.*] Vacaresse, A., D. Boscher, S. Bourdarie, A. Korth, and R. Friedel, Correlations between measurements and numerical simulation results for ring current protons (online pdf version).